JONATHAN T. H. WU

GEOSYNTHETIC REINFORCED SOIL (GRS) WALLS

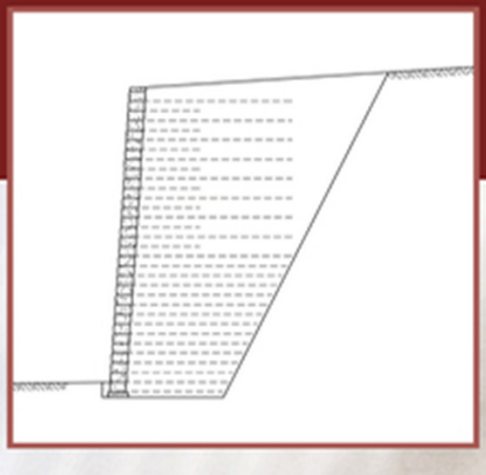

WILEY Blackwell

Geosynthetic Reinforced Soil (GRS) Walls

Geosynthetic Reinforced Soil (GRS) Walls

Jonathan T.H. Wu

Professor of Civil Engineering
University of Colorado Denver
Director of the Reinforced Soil Research Center
Editor-in-Chief of the Journal of Transportation Infrastructure Geotechnology

WILEY Blackwell

This edition first published 2019

Registered Offices
John Wiley & Sons, Inc., 111 River Street, Hoboken, NJ 07030, USA
John Wiley & Sons Ltd, The Atrium, Southern Gate, Chichester, West Sussex, PO19 8SQ, UK

Editorial Office
9600 Garsington Road, Oxford, OX4 2DQ, UK

For details of our global editorial offices, customer services, and more information about Wiley products visit us at www.wiley.com.

Wiley also publishes its books in a variety of electronic formats and by print-on-demand. Some content that appears in standard print versions of this book may not be available in other formats.

Library of Congress Cataloging-in-Publication Data

Names: Wu, Jonathan T. H., author.
Title: Geosynthetic reinforced soil (GRS) walls / by Jonathan T.H. Wu.
Description: Hoboken, NJ : John Wiley & Sons, 2019. | Includes bibliographical references and index. |
Identifiers: LCCN 2017044670 (print) | LCCN 2017056353 (ebook) | ISBN 9781119375852 (pdf) | ISBN 9781119375869 (epub) | ISBN 9781119375845 (cloth)
Subjects: LCSH: Reinforced soils. | Geosynthetics.
Classification: LCC TA760 (ebook) | LCC TA760 .W8 2018 (print) | DDC 624.1/62–dc23 LC record available at https://lccn.loc.gov/2017044670

Cover Design: Wiley
Cover Image: © Alena Hovorkova/Shutterstock
Cover Illustrations: Courtesy of Jonathan T.H. Wu

Set in 10/12pt Warnock by SPi Global, Pondicherry, India

10 9 8 7 6 5 4 3 2 1

Contents

Preface

Since the reintroduction of reinforced soil in the early 1960s, many innovative reinforced soil wall systems have been developed to deal with earthwork construction where an abrupt change in grade is desired or needed. Reinforced soil wall systems deploy horizontal layers of tensile inclusion in the fill material to improve or achieve stability. These wall systems have demonstrated many distinct advantages over their conventional counterparts such as cantilever reinforced concrete earth retaining walls, gravity concrete walls, crib walls, etc. In addition to high load-carrying capacity, reinforced soil walls are typically more ductile (hence less susceptible to sudden collapse), more flexible (hence more tolerant to differential settlement), faster and easier to construct, more adaptable to low quality backfill, require less over-excavation, more economical to construct, and have lower life-cycle maintenance costs. To date, reinforced soil walls are being constructed at a rate of over 100,000 m^2 (in terms of total face area) annually in the U.S. alone.

Modern technologies of reinforced soil walls incorporate metallic strips/mats or synthetic polymeric sheets (termed geosynthetics) as tensile inclusion in the backfill during fill placement. Reinforced soil walls have commonly been designed by considering tensile inclusion as quasi-tieback elements to stabilize the fill material through soil-reinforcement interface bonding, and are collectively referred to as mechanically stabilized earth (MSE) walls. MSE walls with geosynthetics as reinforcement have been referred to as geosynthetic mechanically stabilized earth, or simply GMSE. To date, over 60,000 GMSE walls have been built along highways in the U.S.

Reinforcement spacing used in GMSE walls has been relatively large. This stems from a fundamental design concept that spacing of quasi-tieback elements hardly matters to performance, and that larger spacing would result in shorter construction time. The beneficial effect of deploying geosynthetic reinforcement on tight spacing, however, is gaining increased attention. The significant benefits of close reinforcement spacing were first realized through actual wall construction, and later verified by field-scale loading experiments. It has been shown that close reinforcement spacing will increase considerably the load-carrying capacity and, more importantly, improves stability of the reinforced soil mass. Studies have suggested that the behavior of reinforced soil mass with closely spaced reinforcement can be accurately characterized as soil–geosynthetic composites.

Geosynthetic reinforced soil (GRS) emerged as a viable alternative to GMSE in the early 2000s. GRS takes advantage of soil–geosynthetic interaction by which the

soil mass is reinforced internally. To activate a significant beneficial effect of soil–geosynthetic interaction, reinforcement spacing in GRS is much smaller than in GMSE. Note that in the literature the term "GRS" has sometimes been used for all soil structures reinforced by geosynthetic inclusion without any regard to reinforcement spacing or the design concept.

GRS bears strong resemblance to GMSE, in that both systems are composed of three major components: facing, compacted backfill, and horizontal geosynthetic inclusion. The main difference between the two systems lies in the design concept. GRS considers closely spaced geosynthetic inclusion as a reinforcing element of a soil–geosynthetic composite (hence the term "reinforced" in GRS). GMSE, on the other hand, considers the geosynthetic inclusion as frictional tieback tension members to stabilize potential failure wedges (hence the term "stabilized" in GMSE). Because of this difference, the role of facing for the two systems is also very different. In GRS, the soil mass is *internally* reinforced to form a stable mass. The wall facing serves primarily as an aesthetic façade. It also serves to prevent soil sloughing and as a construction aid. In GMSE, however, facing is a major load-carrying component; if facing fails, failure of the GMSE wall will usually be imminent.

In today's practice, GMSE is enjoying a much wider popularity than GRS. This is in part because there is a lack of understanding of GRS, and in part because GMSE is similar to conventional earth retaining walls in design concept. Most designers are not entirely comfortable with a soil wall that achieves stability through internal reinforcing of the soil behind the wall rather than through the resistance offered *externally* by the facing.

Lately, a number of renowned designers and wall builders have estimated about 5–10% failure rate for GMSE, with a majority being associated with serviceability (i.e., excessive deformation). The National Concrete Masonry Association has also estimated a 2–8% failure rate of various types for GMSE walls. Whether it is structural failure or serviceability failure, the failure rate is much too high compared to other types of earth structures. Studies into the causes of failure have not lead to conclusive solutions to the problem. By employing tight reinforcement spacing to form soil–geosynthetic composites of higher stiffness and ductility, GRS has slowly but gradually affirmed itself as a viable alternative wall system to GMSE. GRS has promised some advantages as a sound wall system of the future, including (i) closely spaced reinforcement of GRS improves fill compaction efficiency and relaxes requirement of stiffness/strength of geosynthetics, (ii) GRS tends to be much less susceptible to long-term creep when well-compacted granular fill is employed, (iii) GRS provides much better seismic stability, and (iv) GRS mass exerts less earth pressure against facing and improves facing stability. Failure of GRS is practically nonexistent as long as well compacted granular fill is used. This is likely because GRS does not rely on the stability of any single structural component (e.g., facing or tension anchors) to maintain overall stability.

This book addresses both GRS and GMSE, with a much stronger emphasis on the former. Details of GMSE have been given by several design guides, such as the AASHTO bridge design specifications, the Federal Highway Administration NHI MSE walls and steepened slopes manual, and the National Concrete Masonry Association design manual. For completeness, this book begins with a review of shear strength of soils (Chapter 1) and classical earth pressure theories (Chapter 2). Chapter 3 addresses the

observed behavior of soil–geosynthetic composites, reinforcing mechanisms of GRS, and GRS walls of different types of facing. Chapter 4 addresses geosynthetics as reinforcement, with emphasis on mechanical properties of geosynthetics, including load–deformation properties, creep properties, stress–relaxation properties, and soil–geosynthetic interface properties. Chapter 5 discusses design concepts of GRS walls and describes a number of prevalent design methods for GRS walls. In addition, recent advances on design of GRS and a new design method incorporating the recent advances is delineated. Design examples for each of the design method are given to help illustrate the design methods. Chapter 6 addresses construction of GRS walls, including construction procedure of GRS walls and general construction guidelines. It is my hope that the civil engineering community will become more familiar with GRS through this book, and makes better use of this novel technology in earthwork construction.

This book would not have been possible without the contribution of many of my colleagues and friends. Foremost is Professor Gerald A. Leonards, who was an inspiration for my lifelong interest in the theories and practice of geotechnical engineering. I must acknowledge Bob Barrett, a true innovator of reinforced soil technology, with whom I have had the privilege to work on many fact-exploring projects over the past three decades. From Bob I leaned many key issues of GRS. I also wish to thank Mike Adams and Jennifer Nicks, two relentless FHWA researchers whose field-scale experiments allowed me to learn the behavior of GRS. I also wish to acknowledge an outstanding wall builder, Calvin VanBuskirk, who had the vision to suggest separation of GRS from GMSE. I am especially in debt to Fumio Tatsuoka, who kindly shared many valuable experimental techniques and his unique experiences during my two sabbatical leaves at the University of Tokyo. Fumio was extremely instrumental for many field-scale experiments of GRS that I was involved in.

I was fortunate to have worked with many outstanding research associates on GRS and related subjects, including (in alphabetical order) Noom Aksharadananda, Daniel Alzamora, Vasken Arabian, John Ballegeer, Bill Barreire, Michael Batuna, Melissa Beauregard, Richard Beck, John Billiard, David Bixler, Harold Blair, Eric Y. Chen, Nick S.-K. Cheng, Nelson N. Chou, Alan Claybourn, Phil Crouse, David Curran, Mark Davis, Gary Dieward, Gene Dodd, Robert Duncanson, Nicolas El-Hahad, Chris Ellis, Egbal Elmagre, Zeynep Erdogen, Barbara Evans, Tony Z-Y. Feng, Seth Flutcher, Brian Francis, Chris Gemperline, Dave Gilbert, Justin Hall, Khamis Haramy, Mark Hauschild, Matthew Hayes, Sam Helwany, Dennis Henneman, Jason Hilgers, Zhenshun Hong, Kanop Ketchart, Elaheh Kheirkhahi, Cassie Klump, Ilyess Ksouri, W.T. Hsu, Kevin Lee, S.L. Lee, K.H. Lee, J.C. Lin, C.W. Ma, Paul Macklin, David Manka, Mike May, Rick McCain, Araya Messa, John Meyers, Greg Monley, Larry Moore, Mike Nelson, James Olson, Jean-Baptiste Payeur, Breden Peters, Thang Pham, John Pierce, Michele Pollman, Xiaopei Qi, Mark Reiner, Zac Robinson, Jerzy Salamon, Brett Schneider, Pauline Serre, Rennie Seymour, Daming Shi, Barry Siel, Saeed Sobhi, C.K. Su, Omar Takriti, Damon Thomas, Sheldon C.-Y.Tung, Alan Tygesen, Mark Vessely, Diane TeAn Wang, Roy Wittenburg, Derek Wittwer, Temel Yetimoglu, and Sam S.-H. Yu.

Finally, I wish to express my gratitude to my mother Umeko to whom I owe everything.

Jonathan T.H. Wu
Greenwood Village, Colorado

1

Stresses and Shear Strength of Soils

In the design of earth structures, good knowledge of shear stiffness/strength of soil is of importance because excessive deformation or failure of earth structures may occur as a result of insufficient resistance to shear stress. This chapter presents a review of shear behavior and shear strength of soils that are relevant to the design of earth structures. We begin the chapter with an explanation of stress at a point, followed by a brief explanation of effective stress and Mohr–Coulomb failure criterion. We then discuss commonly used laboratory and field tests for evaluation of shear behavior and determination of the shear strength of soils. We conclude the chapter with a discussion of the design consideration of the shear strength for soils under different loading conditions.

1.1 Stress at a Point

In engineering analysis and design of structures, *stress* has been proven to be an extremely useful parameter to quantify the effects of internal and external influences on a structure. For earth structures, common influences include external loads, self-weight of soil and water, seepage force, and temperature change. Stress in a body is commonly referred to a plane. Stress on a plane with cross-sectional area A when subjected to a force system denoted F can be evaluated by a simple equation: stress = F/A. This equation, however, is useful only if the force on the given plane is known and if the stress can be approximated as being uniform on that plane. This is generally not the case for a soil mass where the stresses of interest typically occur on a plane other than the plane of load applications, and the stresses may be far from being uniform. To this end, we shall begin the discussion with a review of the *stress at a point*, a subject we were first exposed to when studying "mechanics of materials" as undergraduate engineering students. We shall discuss three topics that will help us gain a better understanding of *stresses at a point*: (a) the concept of stress at a point in terms of stress vector, (b) the computation of stress vector on any given plane by the Cauchy formula, and (c) graphical representation of stress at a point by a Mohr circle and the pole of a Mohr circle. A good understanding of these topics will allow us to gain insights into Rankine analysis, a prevailing lateral earth pressure theory, which we will discuss in detail in Chapter 2.

Geosynthetic Reinforced Soil (GRS) Walls, First Edition. Jonathan T.H. Wu.

1.1.1 Stress Vector

Let us begin by considering an earth retaining wall subjected to concentrated and distributed loads over the "crest" (top surface of a wall), as shown in Figure 1.1(a). Figure 1.1(b) shows a plane cutting through the soil mass behind the wall at point *P*. The force acting over a very small area ΔA on the plane of cut surrounding point *P* is denoted ΔF. If the plan of cut is referred to as the "$\vec{n}$ plane" (i.e., a plane with its outward normal being a unit vector $\vec{n}$; the arrow above the notation "n" is merely a symbol indicating that it is a vector, i.e., it has a magnitude, an orientation, and a sense), the intensity of force at point *P* on the $\vec{n}$ plane can be expressed by a *stress vector* $\overrightarrow{T_n}$ as:

$$\text{stress vector } \overrightarrow{T_n} = \lim_{\Delta A \to 0} \frac{\Delta F}{\Delta A} \tag{1-1}$$

Note that the stress vector can be viewed as the *resultant* of stresses on the $\vec{n}$ plane.

We shall find it convenient to identify two major components of $\overrightarrow{T_n}$ which are perpendicular and tangent to the $\vec{n}$ plane:

$$\text{normal stress } (\sigma) = \text{the component of } \overrightarrow{T_n} \text{ that is normal to the } \vec{n} \text{ plane}$$

$$\text{shear stress } (\tau) = \text{the component of } \overrightarrow{T_n} \text{ that is tangent to the } \vec{n} \text{ plane}$$

The stress vector $\overrightarrow{T_n}$ is therefore a resultant of normal stress σ and shear stress τ on the given plane.

If we had chosen a different plane of cut through point *P*, the stress vector on that plane would generally be different from what we obtained previously. In fact, for every plane passing through point *P*, there will generally be a different stress vector associated with that plane. The number of planes passing through point *P* is infinite; hence, there

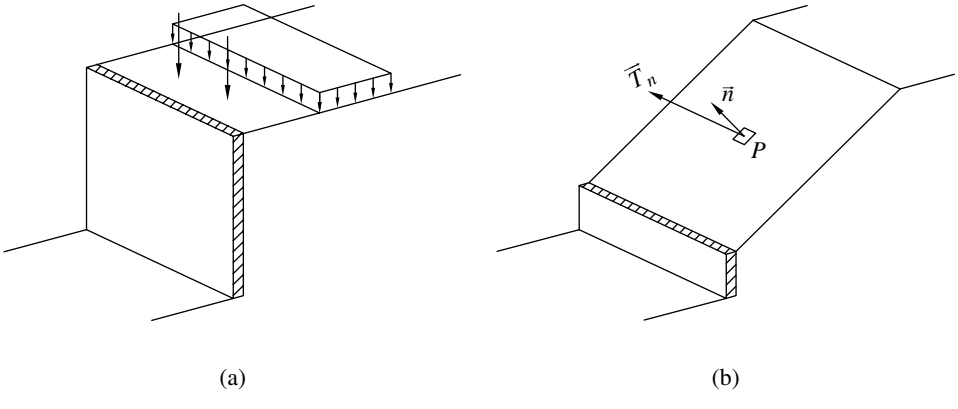

Figure 1.1 (a) An earth retaining wall subjected to self-weight and external loads on the crest and (b) stress resultant $\overrightarrow{T_n}$ on a plane $\vec{n}$ through point *P*

are infinite stress vectors at point *P*. Stress at point *P* is *the totality of all the stress vectors at point P*. To state that we know the stress at a given point, we must know all the stress vectors at that point.

1.1.2 Cauchy Formula

Since there is an infinite number of stress vectors at a point, it would appear that it is not possible to know the stress at a point. This problem was resolved thanks to the *Cauchy formula*. Cauchy (circa 1820) showed that the stress vector on any plane at a point could be determined provided that the stress vectors on three orthogonal planes at that point are known, i.e.,

$$\overrightarrow{T_n} = \overrightarrow{T_n}\, n_x + \overrightarrow{T_n}\, n_y + \overrightarrow{T_n}\, n_z \tag{1-2}$$

where

$\overrightarrow{T_n}$ = the stress vector on a plane with its outward normal unit vector $\vec{n}$

$\overrightarrow{T_x}, \overrightarrow{T_y}, \overrightarrow{T_z}$ = the stress vectors on the *x*-, *y*-, and *z*-planes, respectively

n_x, n_y, n_z = directional cosines of $\vec{n}$ in the *x*-, *y*-, and *z*-directions, respectively, where $n_x = \cos\theta_x$, $n_y = \cos\theta_y$, $n_z = \cos\theta_z$ (see Figure 1.2).

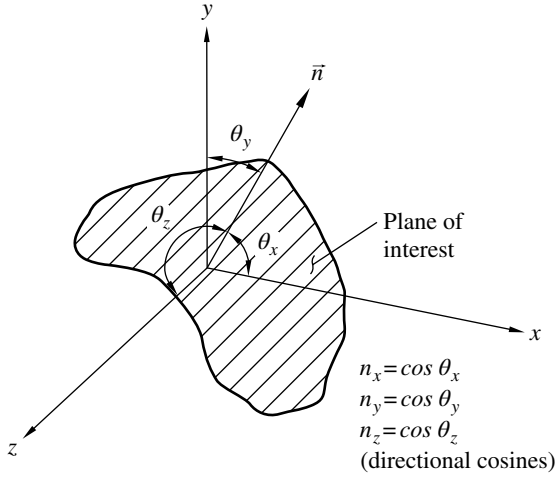

Figure 1.2 Directional cosines of a plane with an outward normal unit vector $\vec{n}$

The Cauchy formula, Eqn. (1-2), allows the stress vectors on any plane to be determined by knowing only the stress vectors on three orthogonal planes; therefore, stress at a point can now be fully defined by knowing only the stress vectors on three perpendicular planes $\overrightarrow{T_x}, \overrightarrow{T_y}$, and $\overrightarrow{T_z}$. As shown in Figure 1.3, $\overrightarrow{T_x}$ can be considered as the resultant of σ_x, τ_{xz}, and τ_{xy}. Similarly, $\overrightarrow{T_y}$ can be considered as the resultant of σ_y, τ_{yz}, and τ_{yx}; and $\overrightarrow{T_z}$, the resultant of σ_z, τ_{zx}, and τ_{zy}.

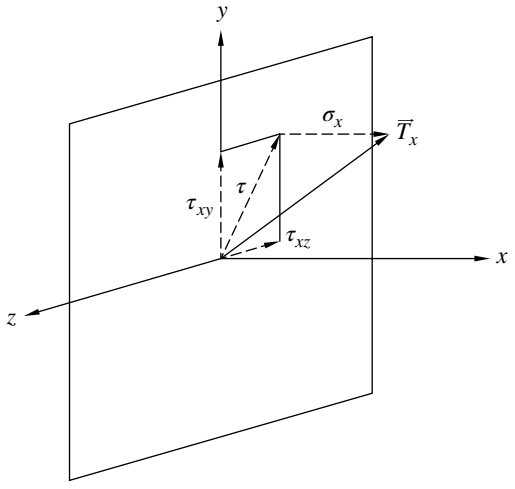

Figure 1.3 Stress vector $\overline{T_x}$ as the resultant of stress components σ_x, τ_{xz}, and τ_{xy}

Since the stress at a point can be defined completely by $\overline{T_x}$, $\overline{T_y}$, and $\overline{T_z}$, it follows that the stress at a point can be described by nine stress components, known as the *stress tensor*:

$$\begin{bmatrix} \sigma_x & \tau_{xy} & \tau_{xz} \\ \tau_{yx} & \sigma_y & \tau_{yz} \\ \tau_{zx} & \tau_{zy} & \sigma_z \end{bmatrix}$$

All of us may have seen a graph like Figure 1.4 in engineering mechanics books whenever the subject of *stress* comes up. The graph shows the nine components of the

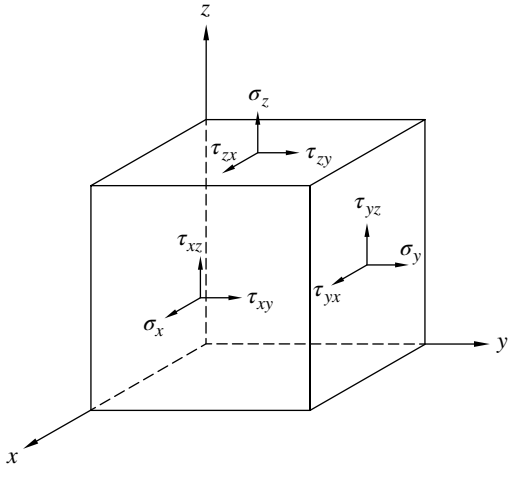

Figure 1.4 Representation of stress at a point by a stress tensor

stress tensor, hence stress at a point. Even though the graph shows the nine components on a cube, we should picture it in our mind as a point. The cube is just a convenient way to show stresses on different planes. With an assumption that the body-moment and couple-stress do not exist in the system, the stress tensor must be symmetrical, i.e., $\tau_{xy} = \tau_{yx}, \tau_{xz} = \tau_{zx}, \tau_{yz} = \tau_{zy}$ (Fung, 1977). The stress tensor therefore has only six independent components.

In a plane-strain condition (see Section 1.4.3), a three-dimensional structure can be analyzed as being two-dimensional. Stress at a point in a plane-strain condition is therefore fully defined if the stress vectors on two orthogonal planes at the point of interest are known (an extension of this statement can be seen in Examples 1.2 and 1.3). The stress tensor in a plane-strain condition can be expressed as:

$$\begin{bmatrix} \sigma_x & \tau_{xz} \\ \tau_{xz} & \sigma_z \end{bmatrix}$$

This stress tensor has three independent stress components ($\sigma_x, \sigma_z, \sigma_{xz}$). If these three stress components are known, stresses on any plane at the point can be determined by the Cauchy formula. For example, the normal stress (σ) and shear stress (τ) on a plane with an outward normal unit vector $\vec{n}$ making an angle θ with the x-axis (as shown in Figure 1.5) can be calculated by:

$$\begin{aligned} \sigma &= \frac{\sigma_x + \sigma_y}{2} + \frac{\sigma_x - \sigma_y}{2}\cos 2\theta + \tau_{xy}\sin 2\theta \\ \tau &= -\frac{\sigma_x - \sigma_y}{2}\sin 2\theta + \tau_{xy}\cos 2\theta \end{aligned} \tag{1-3}$$

Eqn. (1-3) is a simplified form of the Cauchy formula (Eqn. (1-2)) in a two-dimensional condition.

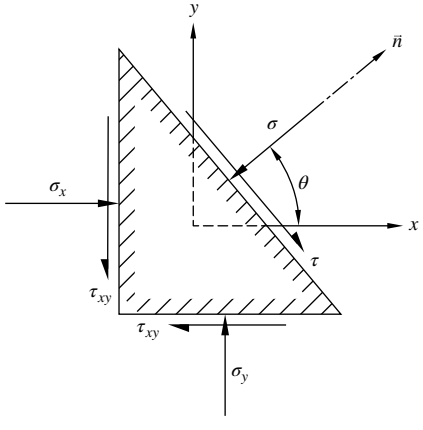

Figure 1.5 Two-dimensional representation of a plane with its outward normal unit vector $\vec{n}$

It should be noted that the use of the concept of stress in the analysis of earth structures is based on an assumption that soil is a continuum. Since soil is in fact a particulate material, in that the particles are typically not bonded and voids are always present, the assumption of a continuum maybe questionable (see Figure 1.6). However, we shall continue to make use of "stress" for the design and analysis of earth structures because it has proven to be an extremely useful tool. Keep in mind, however, that stress in soil is merely a "defined" parameter. When referring to stresses in a soil, it should be viewed on a macro-scale, and the soil is considered a continuum for the purposes of engineering analysis.

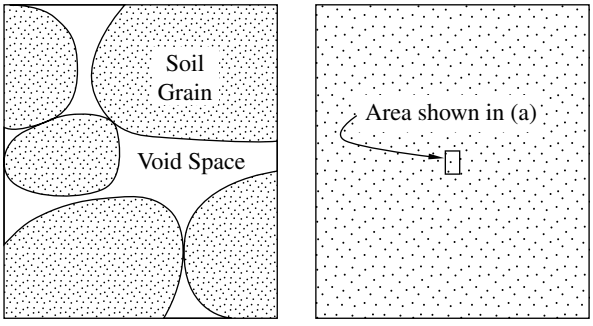

Figure 1.6 Stress at a point in a soil mass: (a) reality (micro-scale) and (b) idealized as being a uniform continuum (macro-scale)

1.1.3 Mohr Circle of Stress

The *Mohr circle of stress*, as shown in Figure 1.7(a), is a plot of normal stress vs. shear stress of all permissible stresses at a point under two-dimensional conditions. Every point on a Mohr circle represents the normal and shear stresses on a particular plane at that point. A Mohr circle of stress therefore can be regarded as a graphical representation of stresses at a point under two-dimensional conditions. There are an infinite number of points on a Mohr circle, and each point corresponds to a plane passing through the point of interest. Two distinct planes exist on a Mohr circle where shear stress $\tau = 0$. These planes are called *principal planes*. The stresses on the principal planes are known as *principal stresses*, denoted by σ_1 and σ_3, as shown in Figure 1.7(a). The principal stress σ_1 is the largest normal stress (or major principal stress), whereas the principal stress σ_3 is the smallest normal stress (or minor principal stress).

Figure 1.7(b) shows the sign conventions for plotting a Mohr circle of stress. In soil mechanics, we denote compressive normal stress as positive and tensile normal stress as negative, which is opposite to the sign convention commonly used in structural mechanics. We do so because soil has little tensile resistance, and most normal stresses in geotechnical engineering analysis are compressive. The sign convention of considering compressive stress as positive avoids having to show nearly every normal stress in geotechnical engineering analysis with a negative sign. A shear stress that makes a clockwise rotation about any point *outside* of the plane is considered a positive shear

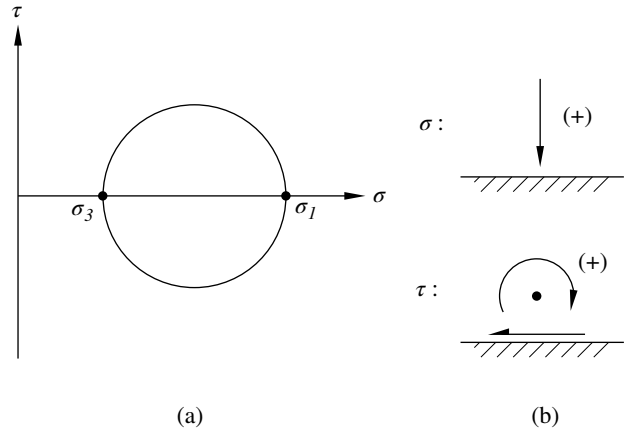

Figure 1.7 (a) Two-dimensional representation of stress at a point by a Mohr circle of stress and (b) sign conventions of normal and shear stresses for plotting Mohr circles

stress (see Figure 1.7(b)). Conversely, a shear stress making counterclockwise rotation about any point outside of the plane is considered a negative shear stress.

1.1.4 Pole of Mohr Circle

We recall that every point on a Mohr circle (with coordinates σ and τ) corresponds to a given plane at the point of interest. It would be very useful to associate the stresses σ and τ with the plane. To that end, the *pole of planes* (or simply *pole*) of a Mohr circle is the most useful. The pole, also referred to as the *origin or center of planes*, is a unique point on a Mohr circle that allows us to determine the orientation of the plane for a given set of permissible σ and τ; it also allows us to determine σ and τ on any given plane.

Once the pole of a Mohr circle is located, we can connect the pole with any point on the circle by a straight line; the orientation of the straight line is then the orientation of the plane. Take a point of coordinates (σ_a, τ_a) on a Mohr circle shown in Figure 1.8(a), for example. The orientation of the plane on which stresses σ_a and τ_a act is indicated by a straight line connecting the pole with point (σ_a, τ_a). Figure 1.8(b) shows the orientation of the two planes of maximum shear stress, each determined by a straight line connecting the pole with the point on the Mohr circle having the largest magnitude of τ. There is one unique plane denoted by a line tangent to the Mohr circle at the pole. The orientation of that tangent line is the orientation of the plane on which the stresses σ_{pole} and τ_{pole} act.

The only question remaining is: how do we locate the pole of a Mohr circle? The answer is simple. There is one and only one pole for each Mohr circle. Therefore, if one permissible set of stress (σ_a and τ_a) and the orientation of the plane of (σ_a, τ_a) are known, the pole can be located by back-tracking the step described above. In other words, all we have to do is draw a straight line through point (σ_a, τ_a) parallel to the given orientation to the plane; the pole of the Mohr circle is the point where the line intersects the Mohr circle. Example 1.1 illustrates how the pole of a Mohr circle of stress is determined. Since $\sigma = 5$ psi and $\tau = 2$ psi (denoted by point A on the Mohr circle) are known to act on the *vertical* plane, a *vertical* line can be drawn through point A to locate the pole of the Mohr circle.

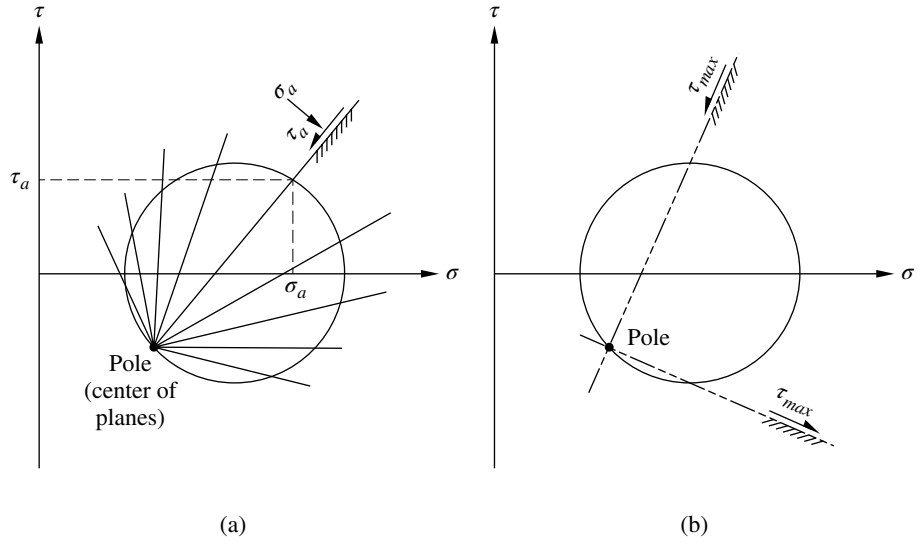

Figure 1.8 (a) The pole of a Mohr circle of stress and (b) orientation of planes of maximum shear stress

Note that the pole can also be located by the stresses on the horizontal plane, $\sigma = 1.5$ psi and $\tau = -2$ psi. Again, there is only one pole for a Mohr circle, so the location of the pole as determined by any sets of σ and τ will be the same. Note that the orientation of a plane deduced from a pole reflects the *actual* orientation of the plane. The orientation can be described by an angle that it makes with the horizontal, the vertical, or any other reference plane.

Example 1.1 The stress at a point under a plane-strain condition is defined by the stresses on the vertical and horizontal planes, as shown in Figure Ex. 1.1(a). Determine, by Mohr circle of stress, (a) the principal stresses and (b) the orientation of the planes of maximum shear stress.

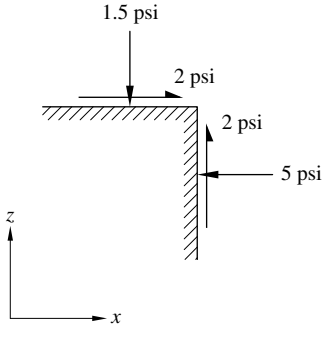

Figure Ex. 1.1(a)

Solution:

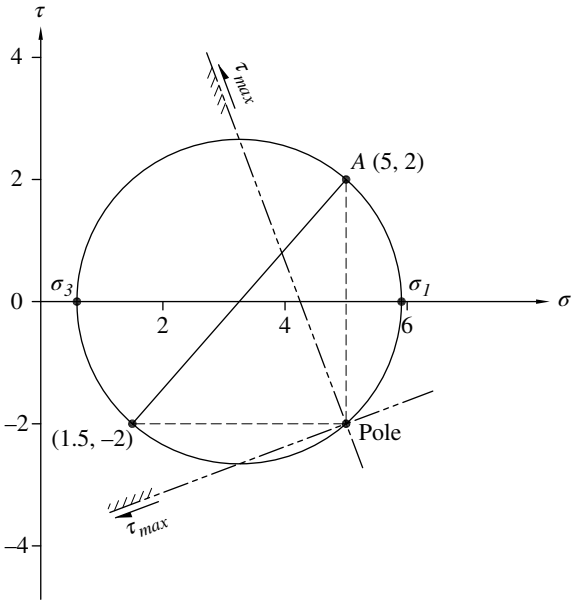

Figure Ex. 1.1(b)

a) The Mohr circle of stress at the point is constructed by the stresses on the two given planes, ($\sigma = 5$, $\tau = 2$) and ($\sigma = 1.5$, $\tau = -2$). From the Mohr circle, the principal stress can be determined graphically as: $\sigma_1 \approx 5.9$ psi and $\sigma_3 \approx 0.6$ psi (note: more precise values can be obtained by sketching the Mohr circle using engineering software, such as AutoCAD).

b) As shown in Figure Ex. 1.1(b), the pole of the Mohr circle can be determined by drawing a vertical line through ($\sigma = 5$, $\tau = 2$) or drawing a horizontal line through ($\sigma = 1.5$, $\tau = -2$). The orientation and respective sense of each of the two τ_{max} planes are as indicated on the Mohr circle, see Figure Ex. 1.1(b).

Examples 1.2 and 1.3 provide additional exercises on how the concept of pole can be used to determine stresses on a plane.

Example 1.2 The stresses on plane A–A and the horizontal plane at the same point are as shown in Figure Ex. 1.2(a). Note that the shear stress on plane A–A is missing. Determine (a) the shear stress on plane A–A, τ_{A-A}, and (b) the magnitude of τ_{max} and the orientation of the planes of τ_{max}, at the point.

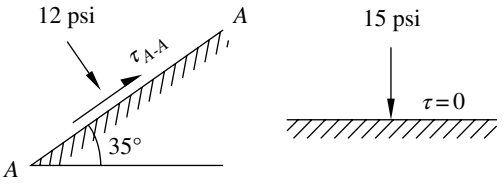

Figure Ex. 1.2(a)

Solution:

A point on the Mohr circle ($\sigma = 15$, $\tau = 0$) corresponding to the horizontal plane is known to be on the Mohr circle, point A. Another point on the Mohr circle corresponding to stresses on plane A–A is along a vertical line through ($\sigma = 12$, $\tau = 0$).

The steps in the solution to (a) and (b) (see Figure Ex. 1.2(b)) are as follows:

i) Sketch a line through ($\sigma = 15$, $\tau = 0$) making an angle $(90° - 35°) = 55°$ from the horizontal (clockwise, toward the general direction of the vertical line through ($\sigma = 12$, $\tau = 0$)); this line will intersect the vertical line (at $\sigma = 12$ psi) at point B, which is also a point on the Mohr circle. The magnitude of τ_{A-A} is the ordinate of point B, hence $\tau_{A-A} = 4.28$ psi.

ii) Construct the Mohr circle with two known points on the circle (points A and B) by first finding the center (determined by the intersection of the horizontal σ-axis and the perpendicular bisector of line $\overline{AB}$). The ordinate of the peak points on the Mohr circle is $\tau_{max} = 4.56$ psi (this can also be determined graphically or from geometric relations in Figure Ex. 1.2(b)).

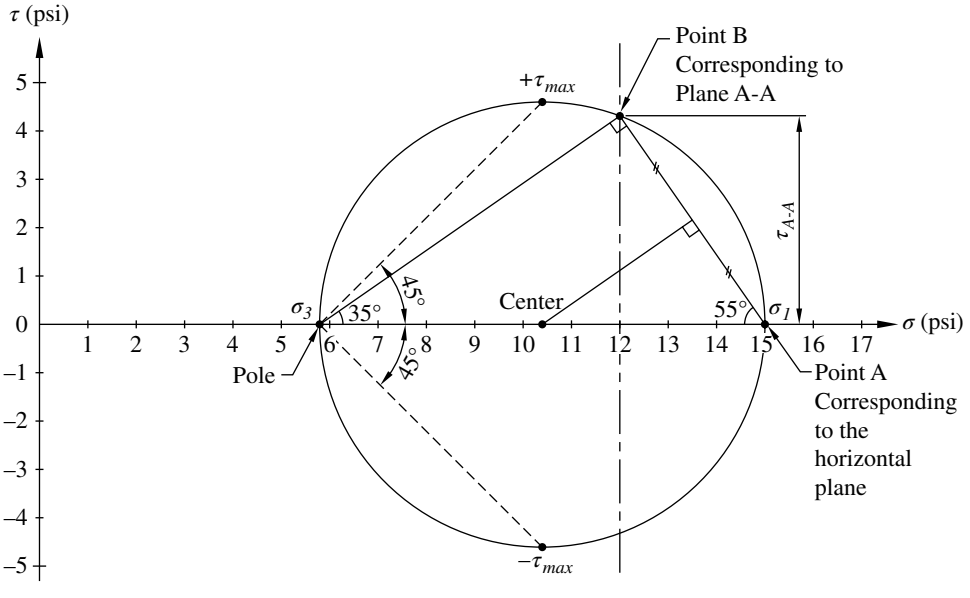

Figure Ex. 1.2(b)

iii) Locate the pole of the Mohr circle by drawing a horizontal line through point A.

iv) Determine the orientation of the two planes of τ_{max}, as shown in Figures Ex. 1.2(b) and (c).

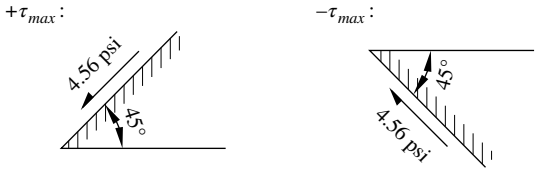

Figure Ex. 1.2(c)

Example 1.3 At a point of interest in a soil mass, τ_{max} is known to be 15 psi, and the stresses on a plane inclined 30° with the horizontal are measured as shown in Figure Ex. 1.3(a). Determine the maximum and minimum normal stresses at point P and the stresses on the 45° plane.

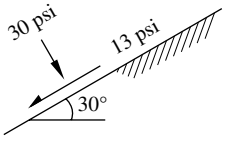

Figure Ex. 1.3(a)

Solution:

The solution can be found by the following procedure (see Figure Ex. 1.3(b)):

i) Locate point P with coordinates ($\sigma = 30$ psi, $\tau = 13$ psi).

ii) Draw a line through point P making an angle of 30° to the horizontal. The line will intersect the horizontal axis at point Q.

iii) Determine the center of the Mohr circle, point A (by connecting points P and Q with a straight line, then sketch a normal line through the midpoint of the line between P and Q; point A will be the intersection between the normal line and the horizontal axis).

iv) Construct the Mohr circle using point A as the center and distance AP or AQ as the radius (this circle is referred to as *Circle A*). The maximum and minimum normal stresses can readily be determined from the Mohr circle; they are the coordinates of the two points where the circle intersects the horizontal axis, σ_1 and σ_3 in Figure Ex. 1.3(b).

v) Locate the pole of the Mohr circle, which turns out to coincide with point Q.

vi) Draw a straight line through point Q making an angle of 45° to the horizontal. The coordinates of the point where the line intersects Circle A are σ and τ on the 45° plane: $\sigma = 22$ psi and $\tau = 15$ psi (as shown in Figure Ex. 1.3(b)).

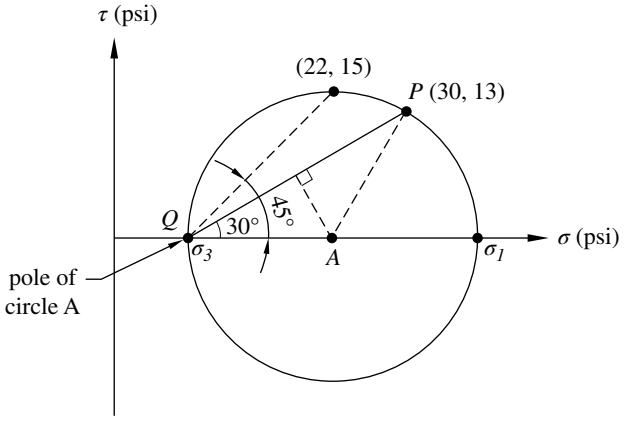

Figure Ex. 1.3(b)

There is another possible scenario where the pole may be located at $\sigma = 30$ psi and $\tau = 13$ psi (i.e., point P). In that case, the Mohr circle will be a circle tangent to the 30° line at point P (as shown in Figure Ex. 1.3(c)). Such a circle will have its center at point B,

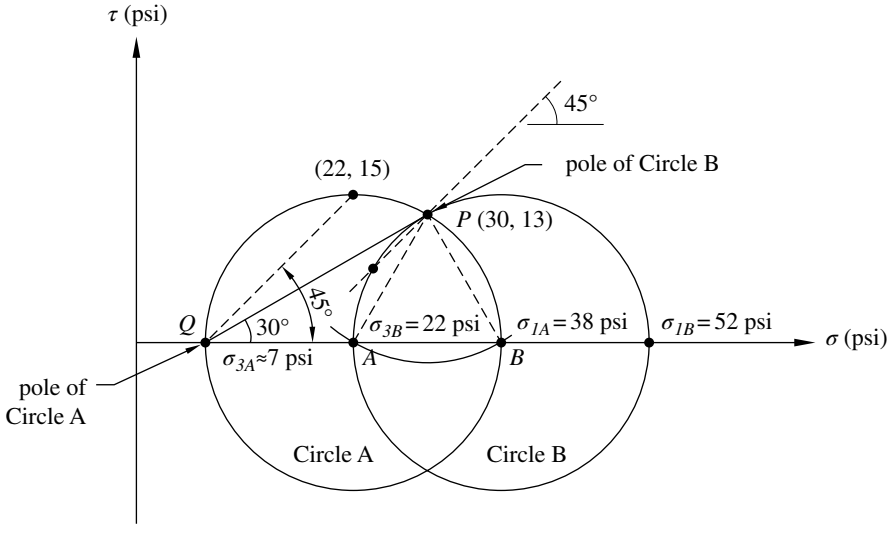

Figure Ex. 1.3(c)

and is referred to as *Circle B*. The maximum and minimum normal stresses are readily determined from Circle B. The stresses on the 45° plane can be determined by sketching a straight line from point P (i.e., from the pole of Circle B) making a 45° angle to the horizontal plane.

From the two Mohr circles seen in Figure Ex. 1.3(c), σ_1 and σ_3 for the two scenarios, as well as respective stresses on the 45° planes, can readily be determined. Their values are shown in Figure Ex. 1.3(d).

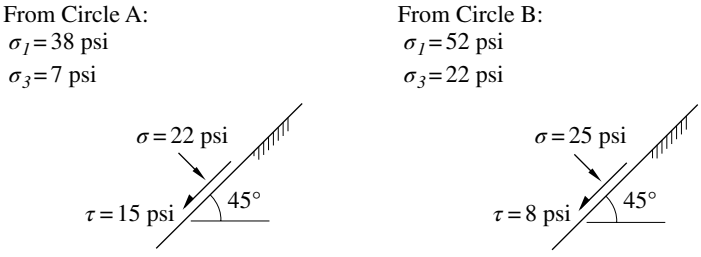

Figure Ex. 1.3(d)

1.2 Concept of Effective Stress

Natural soil is generally a three-phase material, comprising solid particles, pore water, and pore air. Since the pore fluids (pore water and pore air) offer no resistance to static shear stress, the conventional definition of stress has to be revised when dealing with the shear strength of soil. This brings about the concept of effective stress. The effective normal stress, commonly denoted as σ', is the part of applied normal stress that *controls the shear resistance and volume change of a soil* when water is present in the pores. In 1923, Terzaghi presented the principle of effective stress, an intuitive relationship based on experimental data of fully saturated soils. The relationship is:

$$\sigma' = \sigma - u \tag{1-4}$$

where σ is the total stress and u is the porewater pressure. The total stress is the stress calculated by picturing the soil as a single-phase continuum, i.e., the definition commonly used for normal stress.

Although the shear resistance of soil is controlled by effective stress, it is sometimes simpler to perform stability analysis of earth structures in terms of total stress because it does not require us to know the porewater pressure. This, however, is only warranted when a valid relationship can be established between shear strength and total stress. Such a relationship is only available in a limited number of cases where variations of in situ porewater pressure or drainage conditions do not deviate significantly from those in the laboratory tests. The short-term stability of saturated clays is a distinct example where total stress analysis with undrained shear strength can be carried out for stability analysis. This point will be addressed further in Section 1.5.2.

1.3 Mohr–Coulomb Failure Criterion

If shear stress on a plane reaches a limiting maximum value on that plane, shear failure is said to occur. A number of failure criteria for soils have been proposed to define the limiting condition, such as Mohr–Coulomb criterion, triangular conical criteria, extended von Mises criteria, curved extended von Mises criteria (Lade, 2005). Among these failure criteria, the first two have frequently been used for analysis of earth structures conducted by the finite element methods of analysis. The Mohr–Coulomb failure criterion is by far the most commonly used criterion for limiting equilibrium analysis and routine design of earth structures.

In the Mohr–Coulomb failure criterion, the shear strength (τ_f) of soil can be described by the following equation:

$$\tau_f = \sigma_f \tan\phi + c \tag{1-5}$$

in which σ_f is normal stress at failure, ϕ is the *angle of internal friction* (or simply *friction angle*), and c is *cohesion*. Even though Eqn. (1-5) is a common expression of the Mohr–Coulomb failure criterion, it falls short of describing the stresses involved in a rigorous manner. We know from Section 1.1 that stresses are generally different on different planes. However, Eqn. (1-5) only describes the relationship between the normal and shear stresses *at failure*, and does not address the associated plane of the stresses. Yet it has been found to be a useful expression for performing total stress analysis in which the strength of a soil is defined by total stress strength parameters c and ϕ. This point is discussed further in Section 1.5.

A more rigorous expression of Mohr–Coulomb failure criterion is given in terms of effective stress as:

$$\tau_{ff} = \sigma'_{ff} \tan\phi' + c' \tag{1-6}$$

In Eqn. (1-6), the double subscript ff denotes *on failure plane at failure*, τ_{ff} is the shear stress *on failure plane at failure* (commonly referred to as *shear strength*), σ'_{ff} is the effective normal stress *on failure plane at failure*, and c' and ϕ' are effective shear strength parameters. Recall Terzaghi's effective stress principle that the shear resistance of soil is dictated by effective stress, as seen in Eqn. (1-6).

As shown in Figure 1.9, the straight line given by Eqn. (1-6) is a line tangent to all effective stress Mohr circles at failure. Failure is said to occur when the Mohr circle "touches" the straight line, known as the *Mohr–Coulomb failure envelope*. The point of tangency (such as point F in Figure 1.9) represents the effective normal stress and shear stress on failure plane at failure. Note that this is true only when the normal stress is expressed in terms of effective stress. Also note that the failure envelopes for many soils may not necessarily be straight lines, especially for dense soils (dense sands and stiff clays), but a straight-line approximation can be taken over the range of stress of interest. This is discussed further in Section 1.5.1.

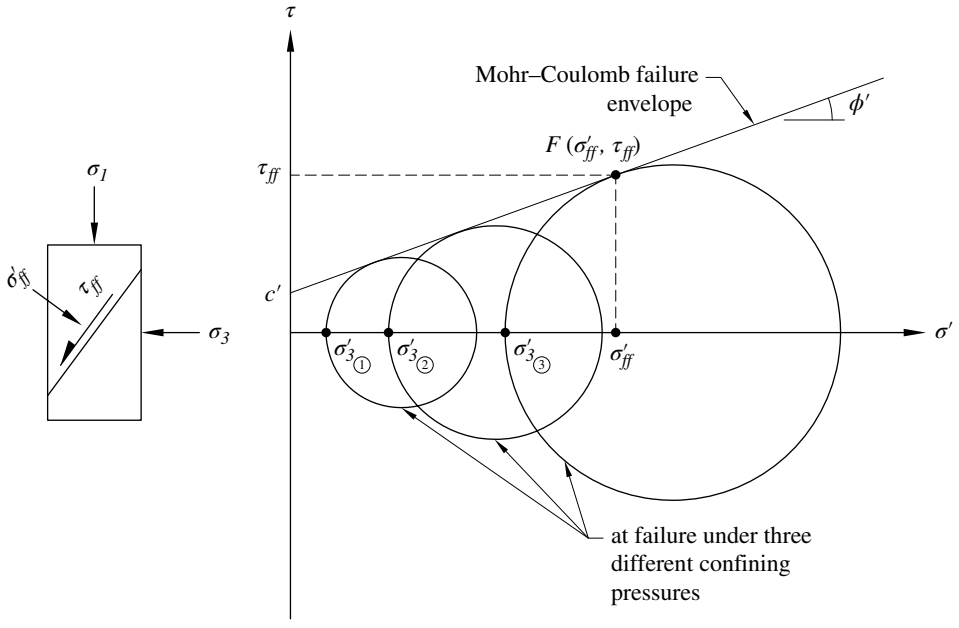

Figure 1.9 The Mohr–Coulomb failure criterion in terms of effective stress, where stresses on the failure plane at failure (σ_{ff}', τ_{ff}) are represented by the point of tangency of the Mohr circle

In terms of principal stresses, the Mohr–Coulomb failure criterion can be expressed as

$$\sigma_{1f}' = \sigma_3' \tan^2\left(45° + \frac{\phi'}{2}\right) + 2c'\tan\left(45° + \frac{\phi'}{2}\right) \tag{1-7}$$

or

$$\left(\sigma_1' - \sigma_3'\right)_f = \frac{2c\cos\phi' + 2\sigma_3 \sin\phi'}{1 - \sin\phi'} \tag{1-8}$$

The subscript *f* in Eqns. (1-7) and (1-8) means "at failure." These equations are useful in some applications of the Mohr–Coulomb failure criterion.

The use of the Mohr–Coulomb failure criterion requires determination of the *Mohr–Coulomb strength parameters* c' and ϕ' (or c and ϕ). It is important to keep in mind that these strength parameters are not "inherent" soil properties. Their values have been found to vary with the drainage condition, stress path, and stress history of a soil.

1.4 Shear Strength Tests

We will now look at some common tests used for determining the shear strength of soils, with emphasis on determination of the Mohr–Coulomb shear strength parameters c' and ϕ' (referred to as *Mohr–Coulomb drained strength parameters*) or c and ϕ

(referred to as *Mohr–Coulomb undrained strength parameters*). The shear strength parameters can be determined by conducting laboratory tests or in situ (a Latin phrase meaning "on site") tests. The most commonly used laboratory tests are the direct shear test, the triaxial compression test, and the unconfined compression test. The most common field tests in North America are the standard penetration test and the cone penetration test. For cohesive soils, vane shear tests have sometimes been used in the laboratory as well as in the field for determination of undrained shear strength.

There is an abundance of literature on shear strength tests (e.g., Bishop and Henkel, 1962; Head and Epps, 1982; Holtz et al., 2011). Only a brief description of commonly used shear strength tests is given here.

1.4.1 Direct Shear Test

Figure 1.10 shows a schematic diagram and a photo of direct shear test setup and apparatus. In direct shear test, a specimen of soil prepared at prescribed density and moisture content is confined laterally in a metal box of a square or circular cross-section. The box is split horizontally in half with a small clearance between the upper and lower boxes. The test is typically carried out by fixing the position of the lower box and applying horizontal forces to move the upper box relative to the lower box. A constant normal load (N) is first applied to the top of the specimen by a dead weight or an air bladder, then the shear force (T) exerted on the upper box is gradually increased until failure occurs. The test is usually repeated with a few different normal loads to determine the Mohr–Coulomb strength parameters c and ϕ.

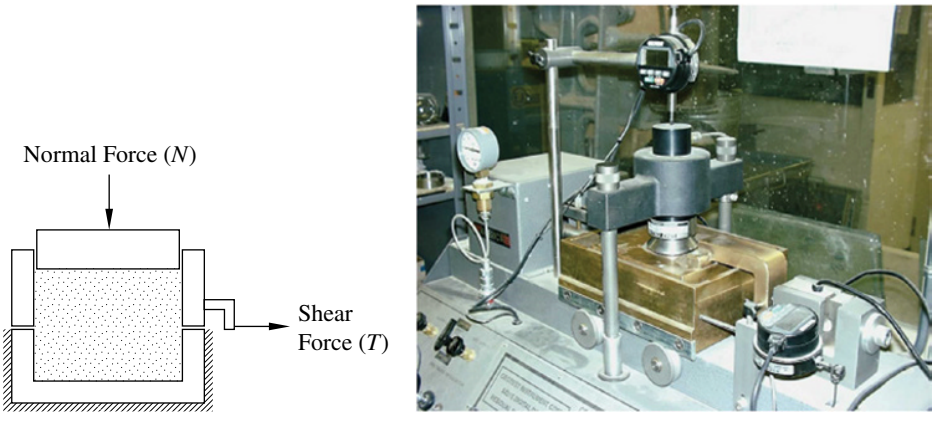

Figure 1.10 Direct shear test: (a) schematic test setup and (b) a photo of test apparatus

A typical set of direct shear test results are shown in Figure 1.11(a). In addition to the relationships between the relative displacements of the upper and lower boxes (δ) and the shear stress (*shear stress* $= T/A$), vertical displacement of the soil specimen